Monte Carlo Studies of Underconstrained Magnetism in Ultracold Fermionic Alkaline Earth Atomic Gases

by

Pavao Santak

A thesis submitted to the faculty of the
University of Colorado in partial fulfillment
of the requirements for the award of
departmental honors in the Department of Physics
2016

This thesis entitled:
Monte Carlo Studies of Underconstrained Magnetism in Ultracold Fermionic Alkaline Earth Atomic Gases
written by Pavao Santak
has been approved for the Department of Physics

_____
Prof. Michael Hermele

_____
Prof. John Cumalat

_____
Ms. Ann Scarritt

Date _____

The final copy of this thesis has been examined by the signatories, and we find that both the content and the form meet acceptable presentation standards of scholarly work in the above mentioned discipline.

Santak, Pavao (B.A., Physics)

Monte Carlo Studies of Underconstrained Magnetism in Ultracold Fermionic Alkaline Earth Atomic Gases

Thesis directed by Prof. Michael Hermele

Physicists have been trying to create artificial magnetic systems using ultra-cold atomic gases as their simulators. However, behavior of many ultra-cold atomic systems is not very well understood yet. Ultra-cold fermionic alkaline earth atomic (AEA) gases are one of those systems.

In this thesis, we study the effects of thermal fluctuations on the overall macroscopic behavior of ultra-cold fermionic AEA gases using a particular semiclassical model. We study the AEA systems on a square lattice with periodic boundary conditions. To investigate the behavior of AEA systems under the effects of thermal fluctuations, we analyze several different types of correlation functions, which correspond to different physical observables. We analyze the correlation functions using the results obtained from Monte Carlo simulations. We show that for the cases studied, all the correlation functions approach zero as the system size goes to infinity at any temperature, indicating that no phase transition occurs as a consequence of thermal fluctuations.

Dedication

To my mum, who weathered the storm in last couple of years and to Srecko Kilic, whose dedication is my inspiration.

Acknowledgements

I would first and foremost like to thank Michael Hermele for providing me with an opportunity to gain research experience in theoretical physics. Your mentorship during the course of this project was far better than I could ever ask for, your amount of guidance and support for was incredible, you further enhanced my interest in theoretical physics, and in particular condensed matter physics and you taught me many things I could have never learned in a regular classroom setting.

I would also like to thank several other professors who played a key role in my academic development - John Cumalat for tremendous advice he has given me throughout my undergraduate career; Shijie Zhong, who was my first physics professor in college, who helped me in getting used to the more advanced way of thinking and tolerated my frequent very basic math questions which were well below the level of knowledge of other students in the class; Andreas Becker, who serves as an inspiration for his love of physics and for passing on that love to his students; and Markus Pflaum, who showed me that abstract mathematics is much more than simply manipulating fancy symbols for the sake of doing so.

Finally, I would like to thank the entire ELLC program at University of Colorado at Boulder for helping me adapt to a completely new surrounding in my early college career and for teaching me how to stay humane even in the most difficult of times.

Contents

Chapter

Appendix

Tables

Table

Figures

Figure

Chapter 1

Background

1.1 Introduction

Experimental advances in atomic and molecular physics in last two decades have opened new frontiers in many body physics. Ever since the observation of Bose Einstein (BEC) in 1995 [2] in a dilute gas consisting of Rb^{87} atoms, the field of experimental many body atomic and molecular physics has grown rapidly. For example, scientists have been able to successfully adjust interactions between the atoms in cold gases [6], which led to the observation of fermionic condensates [19] in 2003. It has also been proposed that ultracold gases in optical lattice potentials can be studied as quantum simulators of various correlated systems [3], while some scientists have also proposed using them in quantum computing [7]. With experimental advances, many new interesting theoretical questions arise. So far, many of those theoretical questions have not been answered.

In this thesis, we address and answer one of those questions. We focus our attention on ultracold fermionic alkaline earth atomic gases and we investigate the effects of thermal fluctuations on their macroscopic behavior. More specifically, we analyze the AEA gases in optical lattice potentials. We look into the semiclassical limit of a Hubbard model in a Mott insulating limit for an ultracold fermionic atomic gas on a square lattice with periodic boundary conditions. We investigate whether fermionic AEA systems spontaneously break any symmetries, in which case a phase transition occurs. To see whether any symmetries are spontaneously broken in AEA systems as a consequence of thermal fluctuations, we will analyze several different correlation functions. In order to analyze correlation functions, we will use the results of Monte Carlo simulations, which

were written and run in Julia programming language [14].

1.2 The AEA model

1.2.1 About the AEA Model

In order to investigate the behavior of AEA systems, we need to specify the energy(Hamiltonian) of the system. To do so, we look into the physical picture of atoms in optical lattice potential. First, each atom has an equal potential energy due to interaction with the lattice, as in this case, atoms are trapped in an optical lattice potential consisting of potential wells of equal depth and width. Naturally, atoms can move so they also have kinetic energy. Kinetic energy of an atom and the potential energy due to interaction with the lattice form the hopping term of the Hamiltonian. Finally, the atoms on the same site in the lattice interact repulsively through their spins, forming an interacting term of the Hamiltonian. Taking those energies into account, but not the others (we neglect any possible interactions between the atoms which are not on the same site to zero) means that our Hamiltonian is a Hubbard model Hamiltonian.

The model we consider is a semiclassical limit of a Hubbard model for fermionic AEA gases in a Mott insulating limit. In a Mott insulating limit, the interaction term is much bigger than the hopping term, so that we can treat the contribution due to hopping terms as a perturbation to the Hamiltonian consisting only out of interaction energies. Here we completely neglect the effects of hopping in order to get the final quantum Hamiltonian. The derivation of the semiclassical Hamiltonian from a quantum Hamiltonian for these systems is described in [13].

The model we analyze is a continuous spin model. As such, its Hamiltonian is described by interactions between magnetic moments of atoms, which are proportional to their spins. In this case, since the elements considered have their s orbital completely filled, we are talking about nuclear spins of atoms. The spins are represented by complex N-dimensional vectors, where $N = 2I+1$ and I represents nuclear spin, which can be as large as $9/2$ for ^{87}Sr. Hamiltonian takes the following form:

$$H = J \sum_{<\vec{i},\vec{j}>} |\hat{n}_{\vec{i}}^{\dagger} \cdot \hat{n}_{\vec{j}}|^2 \tag{1.1}$$

$\hat{n}_{\vec{i}}$ represents a spin at site $\vec{i}$. It is a N-dimensional complex unit vector. Because spins are normalized, but can point in any direction in space, this model is semiclassical. Here, the sum is over neighboring spins (represented in the Hamiltonian by <>). We take the periodic boundary conditions, so that spins on the opposite edges of the square lattice also interact with each other, as long as they take the same horizontal or vertical position in the lattice. J represents the exchange energy between the spins. J is positive so AEA systems interact antiferromagnetically. Since J is equal for any pair of spins, any system in consideration is isotropic.

These systems possess the $SU(N)$ symmetry. $SU(N)$ is a special unitary group of degree N, N being the number of vector components of the spin. Its elements are unitary matrices U, meaning that $U^{-1} = U^{\dagger}$ and $det(U) = 1$. These systems have $SU(N)$ symmetry since if for all the spins $\hat{n}_{\vec{i}}$, $\hat{n}_{\vec{i}} \to U\hat{n}_{\vec{i}}$, where $U \in SU(N)$, the Hamiltonian stays the same.

The probability of the system being in any microstate i with energy E is given by the Boltzmann distribution function

$$P(i) = \frac{e^{-E_i/kT}}{Z} \tag{1.2}$$

,

where k is the Boltzmann's constant, T is the absolute temperature and Z is the partition function, which takes care of the normalization.

1.2.2 Physical Consequences of the Energy Equation

There are a couple of very important physical consequences of the energy equation for the AEA systems. First, we notice that the phase of a vector representing the nuclear spin of an atom is physically irrelevant, as the energy of a system stays the same if $\hat{n}_{\vec{i}} \to e^{i\theta}\vec{n}_{\vec{i}}$ for some position in the lattice $\vec{i}$ and some phase θ. Furthermore, we notice that the energy is minimized when all the

spins are orthogonal to each other. Since there are many ways for all the spins to be orthogonal to each other, especially as the number of vector components of the spin increases, the ground state is not uniquely determined. Such a feature is often seen in geometrically frustrated magnets [18], but in this case it is not the geometry of the lattice that gives rise to multiple ground states; it is the nature of the Hamiltonian. As there are many ways for the system to arrange itself to minimize the energy, AEA systems are said to be underconstrained.

1.2.3 Estimating the Dimension of the Ground State Manifold

Since the ground state is not uniquely determined, the set of all the ground states forms the ground state manifold. Determining the dimension of the ground state manifold provides a useful staring point to think about the possibility of magnetic order developing as a consequence of thermal fluctuations.

To estimate the dimension of the ground state manifold, we use the Maxwellian counting argument. First, we notice that the dimension of the ground state manifold is given by the number of degrees of freedom minus the number of independent constraints ($D = F - K$). Then, since we can think about one complex dimension as two real dimensions, we conclude that any spin in a system can be described by a N-dimensional vector expressed by $2N$ real spherical coordinates. Since there is already a constraint on length of the real and imaginary parts of the vector, we can freely choose $2(N-1)$ angles for each vector representing a spin. Since there are N_s spins in the system, there are in total $F = 2N_s(N-1)$ degrees of freedom. Also, there are two constraints each interaction between spins needs to satisfy. As each interaction is determined by an inner product between two neighboring spins, we can see that for the system in the ground state manifold, both real and imaginary part of each interaction need to be zero. Thus, for each interaction between the spins there are two constraints. Since there are $2N_s$ interactions in the system, there are in total $4N_s$ constraints imposed on the system when it is in the state in ground state manifold. As the number of independent constraints is at most as big as the total number of constraints, we find a lower bound on the dimension of the ground state manifold.

$$D \geq 2N_s(N-3) \tag{1.3}$$

We can see that the lower bound is not particularly useful for the cases $N = 2$ or $N = 3$. However, we observe that due to the extensive dimensionality of the ground state manifold, we are less likely to find magnetic order in the AEA systems, especially for the bigger N cases.

1.3 Spontaneous Symmetry Breaking and Correlation Functions

1.3.1 What is Spontaneous Symmetry Breaking?

The concept of spontaneous symmetry breaking (SSB) is one of the most important concepts in modern physics. It is widely used both in condensed matter physics [20, 22] and in particle physics [9, 8]. SSB is defined as a physical phenomenon in which the equations governing the behavior of the system are symmetric under a symmetry transformation, but the state of the system is not.

As an example of SSB, consider a 2D Ising model with Hamiltonian $H = -J\sum_{<\vec{i},\vec{j}>} n_{\vec{i}} \cdot n_{\vec{j}}$ on a square lattice in the absence of applied magnetic field. Only the neighboring sites interact, J is positive and $n_{\vec{i}}$ represents a spin at site $\vec{i}$, but each $n_{\vec{i}}$ is a scalar with value 1 or -1. Both the Hamiltonian and the state of the system are invariant under a transformation $n_{\vec{i}} \rightarrow -n_{\vec{i}}\ \forall \vec{i}$ above the critical temperature $T = 2.269J/k$. However, below $T = 2.269J/k$, while the Hamiltonian is still invariant under the same transformation, the state of the system is not due to the fact that the system has a nonzero magnetization and flipping the spins would result in changing the magnetization. In SSB the symmetry is broken spontaneously due to the second law of thermodynamics, which states that in a thermodynamic limit and in an isolated system in equilibrium the entropy of that system is always maximized.

In spin models, spontaneously broken symmetry is an indicator of a phase transition. For example, in the same Ising model on a 2D square lattice, the system is in the paramagnetic phase above the critical temperature. Below the critical temperature, the system is in the ferromagnetic phase.

1.3.2 General Features of Correlation Functions in Spin Models

In statistical mechanics, correlation functions are a way of looking for SSB. Different correlation functions correspond to different broken symmetries and thus to different phase transitions.

Correlation functions are expectation values of quantities which depend on distance between the lattice sites. Most generally, a correlation function between objects studied is defined as

$$C(\vec{r}) =< O(\vec{i})O(\vec{j}) > \tag{1.4}$$

O represent objects whose correlations we're studying, $<>$ is a sign for expectation value/mean, $\vec{i}$ and $\vec{j}$ represent the positions of objects on the lattice and $r = |\vec{j}-\vec{i}|$. On the lattice, components of $\vec{r}$ are nonnegative integers. We define a unit distance to be the distance between the two neighboring sites [1] . To analyze whether SSB occurs in a system as a consequence of thermal fluctuations, we look into limiting behavior of correlation function and vary temperature. We take the system size to infinity and we look for the limiting value of the correlation function as the distance between the lattice sites approaches infinity at some fixed value of temperature. If the limiting value is zero, the system is disordered at that temperature and if the limiting value is a nonzero constant the system is ordered at that temperature.

1.3.3 The Structure Factor

It is often hard to determine limiting behavior of the correlation function we analyze. In a spin system with antiferromagnetic interactions the correlation function might not have limiting behavior. In that case, we perform the discrete Fourier transform of the correlation function. For a square lattice of length L with L even and with periodic boundary conditions, if a correlation function is $C(\vec{r})$, with $\vec{r}$ being the distance between the spins in the lattice,the discrete Fourier transform of the correlation function is

$$C(\vec{q}) = \sum_{\vec{r}} e^{-i\vec{q}\cdot\vec{r}} C(\vec{r}) \tag{1.5}$$

[1] Horizontally and vertically neighboring sites

with $\vec{q} = (q_x, q_y)$ and $q_x = \frac{\pi l_x}{L}$,$q_y = \frac{\pi l_y}{L}$. Also, $l_x \in \{\frac{-L}{2}, \frac{-L+1}{2}, \ldots, \frac{L}{2}\}$ and $l_y \in \{\frac{-L}{2}, \frac{-L+1}{2}, \ldots, \frac{L}{2}\}$. Since $C(\vec{q})$ is complex valued, it has a magnitude and a phase. However, we are only interested in magnitude of $C(\vec{q})$. $|C(\vec{q})|$ is called a structure factor. It tells us how much certain spatial angular frequencies in x and y direction contribute to the correlation function. We are also interested in the error of the structure factor. The error of $C(\vec{q})$ (the standard deviation of the mean) is independent of $\vec{q}$ and is given by

$$Er(\vec{q}) = \sqrt{\sum_{\vec{r}} Er^2(\vec{r})} \tag{1.6}$$

Naturally, the error in structure factor is going to be smaller that the error of $C(\vec{q})$. However, as we will see in the upcoming chapters, overestimating the error doesn't make any difference for these systems.

In analyzing the structure factor, we look for the peaks in the 2D structure factor plot at a fixed temperature. We study different system sizes to investigate existence of peaks corresponding to different spatial angular frequencies. If a peak or peaks diverge as the system size goes to infinity, the correlation function doesn't approach zero in the limit of an infinite system size and the system shows some sort of order. Otherwise, the system is disordered at that value of temperature. If the system is disordered at the temperature studied, we proceed to look for the values of temperature where the peaks of the structure factor diverge, and if we don't find any, the correlation function we are analyzing is zero in the limit of an infinite system size at all the values of temperatures and the system doesn't show order which that correlation function describes. If we find a diverging peak, we again study different temperatures, but now we are looking for the temperatures where the peaks don't diverge so that we can find the critical temperature. Since AEA systems are antiferromagnetic, we will use the structure factor extensively to describe their response to thermal fluctuations.

Chapter 2

The Monte Carlo Approach for the AEA Systems

2.1 Introduction

Monte Carlo method is used commonly in condensed matter physics. As behavior of many systems cannot be described analytically, one needs to describe them numerically, and Monte Carlo is a proven method when extracting behavior of various systems numerically. We use the Monte Carlo method to simulate the dynamics of the system we're interested in. We specifically use Monte Carlo simulations to study the correlation functions. In analyzing the correlation functions using the Monte Carlo simulations, we will use natural units. In other words, we set $J = 1$,$k = 1$ and set units of temperatures in terms of J/k. Of course, when dealing with numerical simulations, one cannot take the system size to infinity, but that is not necessary anyways, as one can draw conclusions from results obtained by analyzing a large enough system size.

In order to efficiently simulate the behavior of the system of interest, we need to use an appropriate algorithm. That is often the biggest challenge with Monte Carlo simulations. In our case of interest, any algorithm we use has to be able to efficiently explore all the possible microstates at a certain temperature T by attempting appropriate transitions from one microstate to another microstate. To efficiently explore all the microstates, any algorithm we use in a simulation has to satisfy two conditions; detailed balance condition and ergodicity.

Detailed balance is a fundamental concept in Monte Carlo simulations. It connects the probability of being in a state to the probability of transitioning to a different state. For any two states a and b and probabilities of being in the state a, $P(a)$ and state b, $P(b)$ the detailed balance

condition states that

$$P(a)T(a \to b) = P(b)T(b \to a) \tag{2.1}$$

where $T(a \to b)$ is the probability of transitioning from state a to state b. Transition probability from state a to state b is always equal to the following:

$$T(a \to b) = min(1, \frac{P(b)}{P(a)}) \tag{2.2}$$

In the case of AEA systems, this means that if a system is in state a and we attempt a transition to state b, the transition probability is

$$T(a \to b) = min(1, e^{\frac{-(E_b - E_a)}{kT}}) \tag{2.3}$$

The other condition a successful Monte Carlo algorithm needs to satisfy is ergodicity. An algorithm is ergodic if starting from any state a we can reach any other state b by running a Monte Carlo simulation. As we will see in the next section, it is often the case that an algorithm is ergodic in theory, but in practice it is very difficult to reach many states starting from a provisional state.

2.2 First Algorithm

First algorithm used in simulations is very useful as a staring point for the analysis of effects of thermal fluctuations on behavior of AEA systems. We can use it to explore the behavior of AEA systems at high temperatures (down to $T = J/k$) and it is used as a check of validity of any future algorithms.

In order to produce an algorithm, we have to generate the state b which we will consider as a new possible state of the system. To generate a state b, we first generate a random spin $\hat{s}$ on a complex N-hypersphere. Since our algorithm needs to satisfy the detailed balance condition, we want to produce a uniform probability density function on the hypersphere. To do so, we use Gaussian random numbers with mean 0 and standard deviation 1 for each component (and thus

we choose 2N Gaussian random numbers). We then normalize a randomly generated spin. After normalizing a randomly generated spin, we choose a random position in the lattice $\vec{i}$ and replace the spin at that random position ($\hat{n}_{\vec{i}}$) with a newly generated spin $\hat{s}$ (Figure 2.1). Now we finished generating a new state b. To attempt a transition to state b, we calculate the difference between energies of original state a and potential new state b and then use the expression for the transition probability for AEA systems (equation2.3) to find a transition probability. If transition probability is 1, we accept the move. If transition probability is less than 1, we generate a uniformly distributed random number between 0 and 1. Then we compare the transition probability to the randomly generated number. If transition probability is bigger than the generated random number, we accept the Monte Carlo move and we are in state b now; otherwise, we reject the move and stay in the original state.

While this algorithm is ergodic, most of the moves will be rejected at low temperatures. On average the energy difference is going to be much bigger than the temperature. Hence, we cannot efficiently explore the states around the ground state manifold with this algorithm. We will need a new, more efficient algorithm to analyze the low temperature behavior of AEA systems.

2.3 Second Algorithm

2.3.1 Vector Projection Onto a Vector Space

To efficiently explore the ground state manifold, we want to generate state b such that its energy is very close to the energy of state a at low temperatures. To generate such a state, we take advantage of vector projection onto a vector space.

Vector projection onto a vector space is a generalization of a vector projection onto another vector. In order to find the vector projection onto a vector space, first suppose that we have a set of N-dimensional complex vectors $\{\vec{a}_i\}$ which span a certain space $S \subset \mathbb{C}^N$. Since a spanning set could always be shrunk to a basis, we can find a basis for S $\{\vec{b}_i\}$. Every element $\vec{d} \in S$ can now be represented as a linear combination of basis elements of S, which can be expressed by the equation

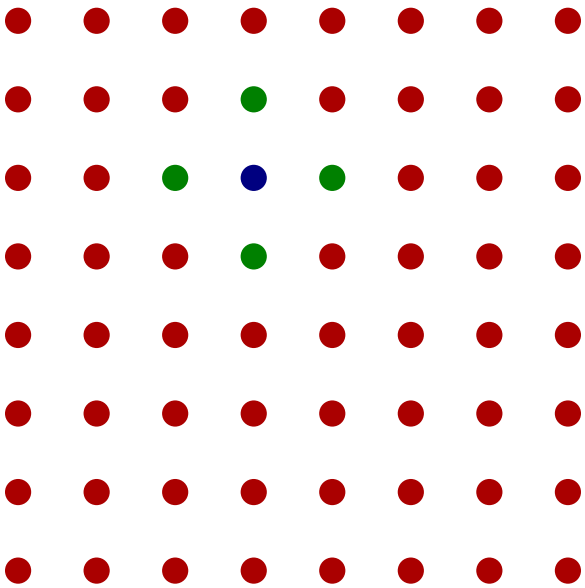

Figure 2.1: Choosing a random spin in the lattice. Blue dot represents the randomly chosen spin while green dots represent its neighbor interacting spins

$$\vec{d} = A\vec{c} \tag{2.4}$$

where column vectors of A are the basis vectors $\vec{b}_i$ and entries of $\vec{c}$ are complex valued constants.

Now we postulate that any vector $\vec{v} \in \mathbb{C}^N$ can be written as a sum

$$\vec{v} = \vec{u} + \vec{w} \tag{2.5}$$

where, $\vec{u} \in S$ and $\vec{w} \in S^{\perp}$. Since $\vec{w} \in S^{\perp}$

$$\vec{d}^{\dagger} \cdot \vec{w} = 0 \tag{2.6}$$

for any $\vec{d} \in S$. Thus

$$A^{\dagger}\vec{w} = 0 \tag{2.7}$$

Using the equation for $\vec{v}$, we conclude that

$$A^{\dagger}\vec{v} = A^{\dagger}\vec{u} \tag{2.8}$$

Now we can find $\vec{u}$ in terms of $\vec{v}$. Using the expression $\vec{u} = A\vec{c}$, we apply $A^{\dagger}$ to both sides of the above equation to get

$$A^{\dagger}\vec{v} = A^{\dagger}A\vec{c} \tag{2.9}$$

Since the columns of A are linearly independent, $A^{\dagger}A$ is invertible and thus

$$\vec{c} = (A^{\dagger}A)^{-1}A^{\dagger}\vec{v} \tag{2.10}$$

Plugging back the expression for $\vec{c}$ into an expression for $\vec{u}$, we get the following final equation:

$$\vec{u} = A(A^{\dagger}A)^{-1}A^{\dagger}\vec{v} \tag{2.11}$$

We note that in our case of interest, we always have a basis for a subspace S whenever we choose four neighbor interacting spins (on a square lattice) for N bigger than 3. Since the vectors are always going to be linearly independent due to the way computer generates them, they always form the basis for their own spanning vector space S.

2.3.2 Algorithm Description

This algorithm efficiently explores the states around the ground state manifold for cases when $N \geq 6$. It is still a local spin move, but is nonetheless very efficient in getting us consistent results down to very low temperatures.

As before, we want to generate a new state b which we will consider as a possible new state of the system. To generate a new state b we first choose a random position $\vec{i}$ on the lattice as before(Figure 2.1). Then we construct a matrix A using the four neighbor interacting spins of a randomly chosen spin $\hat{n}_{\vec{i}}$ in the lattice as column vectors. We split the randomly chosen spin into a projection onto a space spanned by four neighbor interacting spins and the component orthogonal to that space. Spin projection onto a subspace S of $\mathbb{C}^N$ spanned by the neighbor interacting spins is given by

$$proj_S\hat{n}_{\vec{i}} = A(A^{\dagger}A)^{-1}A^{\dagger}\hat{n}_{\vec{i}} \tag{2.12}$$

Then, we calculate the norms of the projection and the orthogonal components. We generate a new random spin $\hat{s}$ as we did in the first algorithm and we also split it into a projection and orthogonal part onto a subspace spanned by column vectors of A. We then normalize the orthogonal and projection parts. To make the difference between energies of states b and a very small, we use the norm of an orthogonal part of the spin in the lattice ($orth_S\hat{n}_{\vec{i}}$) to find the magnitude to orthogonal part of $\hat{s}$. We let $|orth_S\hat{s}| \in (|orth_S\hat{n}_{\vec{i}}| - \epsilon, |orth_S\hat{n}_{\vec{i}}| + \epsilon)$, where ϵ can be chosen

arbitrarily. Then, if $|orth_S\hat{s}| \leq 1$, we attempt a Monte Carlo move as before, using the expression for the transition probability (equation2.3). Note that since $|orth_S\hat{s}|^2 + |proj_S\hat{s}|^2 = 1$, finding the magnitude of an orthogonal part determines the length of the projection two, and since the overall phase doesn't matter, we can choose the values of magnitudes $|orth_S\hat{s}|$,$|proj_S\hat{s}|$ to be the value of components in direction orthogonal to S and in direction of projection onto S. If $|orth_S\hat{s}| > 1$ then the state b is not the state representative of the AEA model as $\hat{s}$ is not a unit vector anymore, so we reject the move automatically.

Since the upper bound on the energy difference between states a and b can be made as small as we want by changing the length of an interval centered around $|orth_S\hat{n}_{\vec{i}}|$, we can use this algorithm to efficiently explore the states around the ground state manifold. However, this algorithm is not completely general. On a square lattice, as there are 4 neighbor interacting spins for each spin, as long as N is smaller than 5, neighbor interacting spins span entire $\mathbb{C}^N$. As $S = \mathbb{C}^N$, we can take no advantage of the vector projection onto a subspace in those cases. When $N = 5$, vectors are linearly independent and we can in principle use this algorithm, but it will not be very efficient. Since there is only one complex axis (a plane) not being spanned by the neighbor interacting spins, we cannot explore the ground state manifold efficiently, as we will reject most of the moves at low temperatures. Hence, we will use this algorithm only for cases when $N = 6, 7, 8, 9, 10$.

2.4 Monte Carlo and Measurement

When running a Monte Carlo simulation, we have to pay attention to the way we calculate the quantities of interest. In particular, we have to make sure that our measurements are independent and represent the actual dynamics of the system.

2.4.1 Equilibration time

When simulating the dynamics of the AEA systems using Monte Carlo simulations, we have to pay attention to initial conditions of the system. Every time when we start a simulation, we have to generate an initial microstate of the system. We can choose that microstate to be a specific state

or we can choose it to be completely random. In any case though, initial state is highly unlikely an indicator of the dynamics of the system. Hence, if we take any measurements at a time step sufficiently close to the initial time of the simulation, the measurement is going to be useless.

In order to take measurements properly, we do not take any measurements for a certain number of moves. The number of moves we have to wait before taking any measurements in order to simulate the dynamics of the system efficiently is called equilibration time. It depends on the specifics of the system (system size, Hamiltonian) and the algorithm we are using.

The easiest way to determine the equilibration time in spin models is by analyzing the energy per spin as a function of time. When the energy per spin equilibrates, the system equilibrates too and we can start taking measurements(Figure 2.2). Naturally, one will still see the fluctuations of energy/spin, but one will not see the change in its average behavior.

2.4.2 Independence of Measurements

When we measure a certain quantity we are interested in related to an AEA system in a Monte Carlo simulation and we look for its expectation value and its error, we have to make sure measurements are uncorrelated in order to correctly calculate the mean and the error in quantity we are interested in. Thus, we won't take measurements every Monte Carlo step, as they will not be uncorrelated. The more time steps the measurements are apart the more independent they are from each other.

However, the measurements are still not completely uncorrelated. To make them uncorrelated, we split the measurements into several blocks. Then we calculate the mean value of a quantity we are interested in for each block and we treat that value as a single measurement.

We have to be careful with the size of each block (the number of data points in it), as too small of a block will still not make our measurements uncorrelated. However, as long as we have an efficient Monte Carlo algorithm and we use a large enough block, this is not an issue. For example, if we use a block which has several times more data points than there are spins in the lattice and we use an algorithm in which the move is accepted every couple of moves, the measurements are

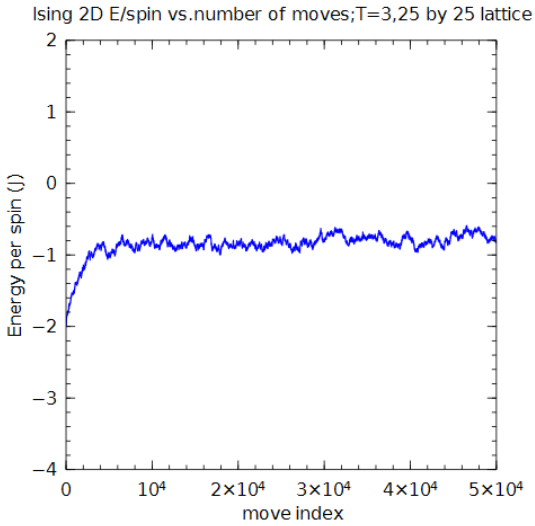

Figure 2.2: Looking for equilibration time using the Energy/spin. We can see that the system equilibrates approximately after about 5000 Monte Carlo moves

going to be uncorrelated.

Chapter 3

Spin Correlation Function

3.1 Introduction

Spin correlation function is a type of correlation function which determines whether the system is magnetically ordered or not. In the AEA model, a nonzero spin correlation function indicates indicates the spontaneous breaking of the $SU(N)$ symmetry and the phase transition from paramagnetic to the antiferromagnetic phase. However, due to extensive ground degeneracy, the phase transition would not be exactly the same one often observed in antiferromagnetic materials. Such a phenomenon is called "order by disorder" and is explored in the next section.

3.2 Order by Disorder

In studying the spin correlation function, we do not look for a phase transition found in the Ising Model or the XY model. That occurs due to the extensive ground state degeneracy of the AEA systems. In systems with extensive ground state degeneracy, a system can prefer certain ground states. As for any temperature a system is most likely found in the macrostate which minimizes the Helmholtz free energy of the system $F = U - TS$, it can happen that most microstates that minimize F at temperature T close to the $T = 0$ are fluctuations about only a finite number of ground states(Figure 3.1).

In that case such a system is often ordered at some temperature close to the zero temperature, even if it might not be ordered at zero temperature. Eventually, as we increase the temperature, the order will be broken. However, the order was preserved (or introduced) by increasing temperature,

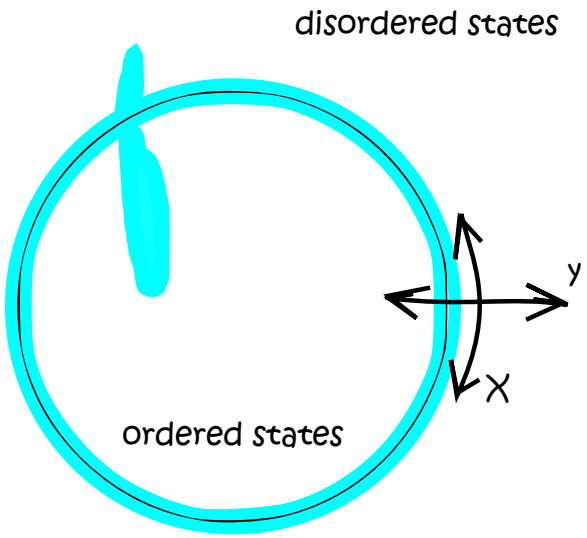

Figure 3.1: Order by disorder. The set of all the point on the circle (x coordinate) represents the set of all the ground states. Space outside of the circle represents the disordered states and space inside the circle represents the ordered states. Set of all blue points represents the fluctuations around the ground state manifold. Since most of the states around the ground state manifold are fluctuations about only a small number of ground states and most of those states are ordered, the system is ordered around the ground state.

which is usually associated with breaking the order.

3.3 Definition

In spin systems, spin correlation function is usually defined as

$$C_s(\vec{r}) =< \hat{n_{\vec{i}}}^{\dagger} \cdot \hat{n_{\vec{j}}} > \tag{3.1}$$

However, we can instantly see that the regular definition will not be of any use in analyzing the AEA systems. As the phase of a vector representing a nuclear spin of an atom does not have any physical significance, the spin correlation function defined above is always going to be zero. Therefore, we study the following function which is going to give us the same information a usual definition of spin correlation function would

$$C_s(\vec{r}) =< |\hat{n_{\vec{i}}}^{\dagger} \cdot \hat{n_{\vec{j}}}|^2 > -\frac{1}{N} \tag{3.2}$$

3.4 Results

Using the mathematical definition of the spin correlation function and the results Monte Carlo simulations, we describe the spin correlation function in the AEA models for the cases which we can efficiently study using the second algorithm.

We notice that for $N = 6$ peaks only show at $\vec{q} = (-\pi, \pi)$(Figure 3.2)

However, the peaks don't increase significantly as a function of temperature and they do not diverge as a function of the system size (Figure 3.3).

Thus, AEA systems is magnetically disordered at all temperatures for $N = 6$. We obtain similar results for $N = 8$(Figures 3.4, 3.5) and for all other values studied.

We conclude that the AEA systems do not show magnetic order as a consequence of thermal fluctuations for $N = 6, 7, 8, 9, 10$.

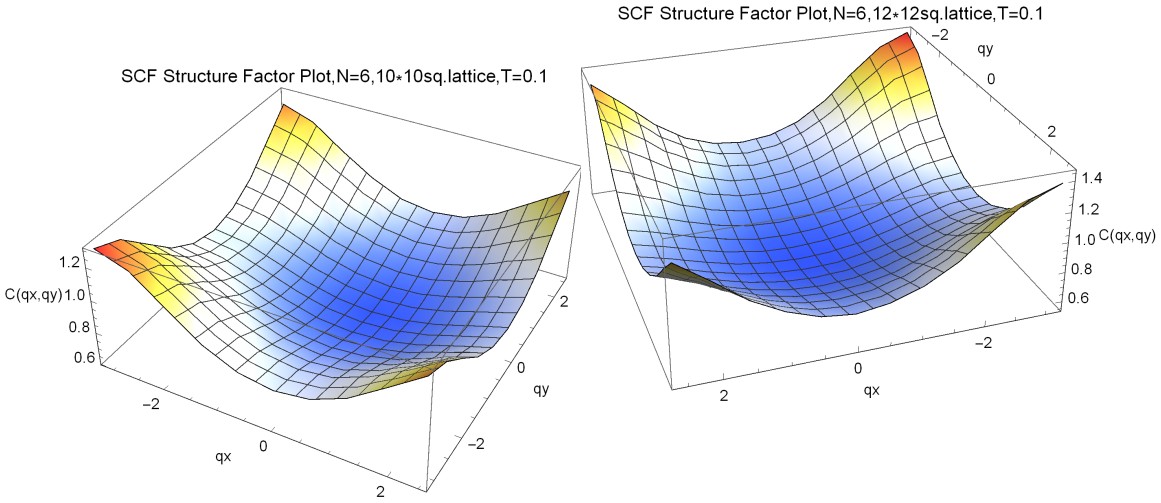

Figure 3.2: Structure factor plots for N=6 at T=0.1 for a 10 by 10 lattice(left) and a 12 by 12 lattice(right)

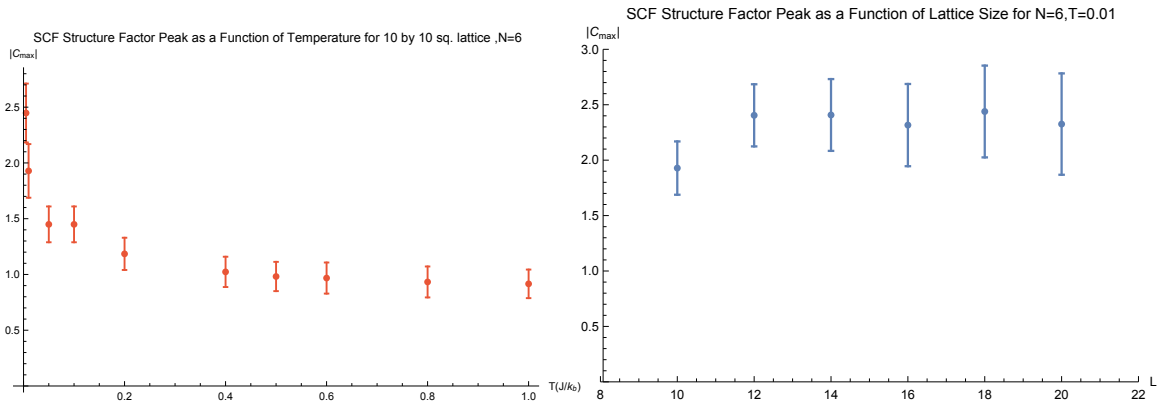

Figure 3.3: Maximum of the structure factor for N=6 as a function of temperature(left) and as a function of system size(right)

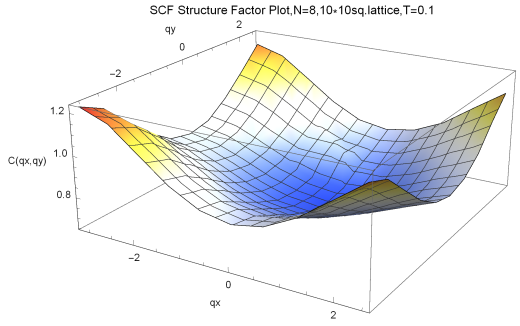

Figure 3.4: Structure factor plot for N=8 at T=0.1 for a 10 by 10 lattice

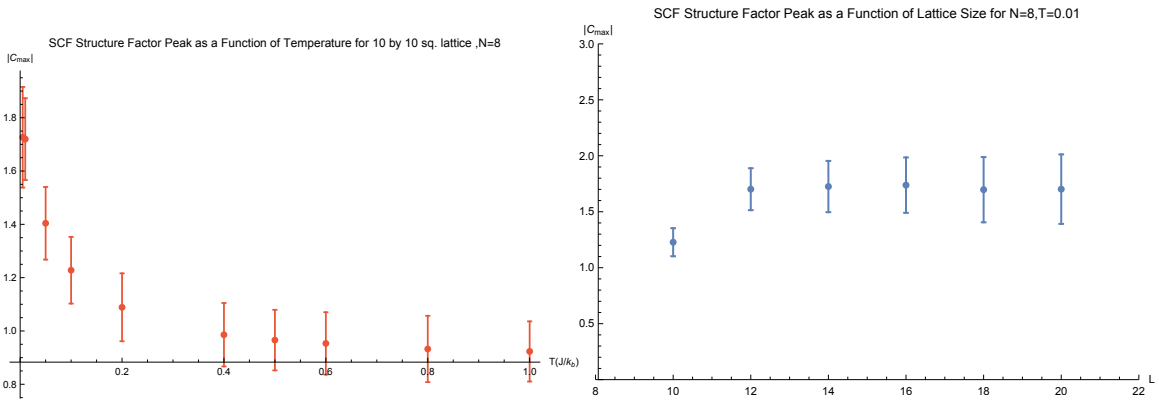

Figure 3.5: Maximum of the structure factor for N=8 as a function of temperature(left) and as a function of the system size(right)

Chapter 4

Bond Correlation Function

4.1 Introduction

The next type of correlation function we look into is the bond correlation function. It describes the correlations between the valence bonds of different atoms in a system. A nonzero bond correlation function indicates breaking of various symmetries of the lattice, such as rotation symmetry or translation symmetry.

4.2 Definition

We can consider vertical and horizontal bonds as objects whose correlation we will study. Without loss of generality, we will consider horizontal bonds. The bond correlation function is then defined as

$$C_b(\vec{r}) =< |\hat{n_{\vec{i}}}^{\dagger} \cdot \hat{n_{\vec{j}}}|^2 |\hat{n_{\vec{k}}}^{\dagger} \cdot \hat{n_{\vec{l}}}|^2 > \tag{4.1}$$

Here, $\vec{i}$ and $\vec{j}$ are horizontally neighboring spins, $\vec{k}$ and $\vec{l}$ are also horizontally neighboring spins, while $\vec{r} = \vec{j} - \vec{i}$. Since both inner products are nonnegative, we will see a nonnegative correlation function for all distances. It seems like this function is not well defined. However, we can still see the behavior of the function in the structure plot, but our analysis is going to be slightly different. Rather that looking for any peaks in the structure plot, like we usually do, we look for the peaks away from $\vec{q} = \vec{0}$.

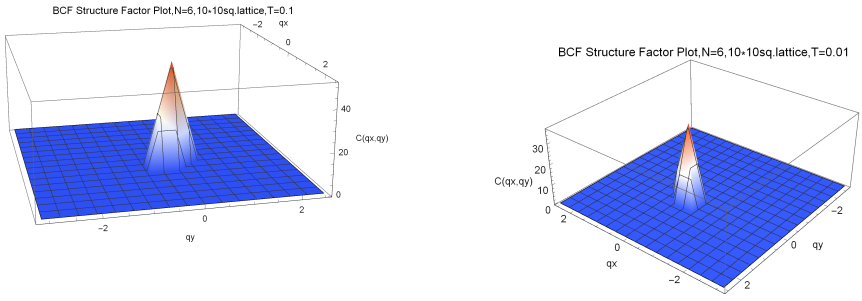

Figure 4.1: Structure factor plots for bond correlation function for N=6 and 10 by 10 lattice

We will also normalize the correlation function. While it is not necessary to do so to find bond order,it is still useful as we usually think of correlation functions as mathematical objects taking values between -1 and 1. In this case, since the neighbor interacting spins are almost orthogonal to each other at low temperatures, the value of bond correlation function is going to be very small at lower temperatures. To normalize the correlation function, just divide it by its maximum value at $\vec{r} = \vec{0}$. Our final correlation function is then

$$C_{bb}(\vec{r}) = C_b(\vec{r})/C_b(\vec{0}) \tag{4.2}$$

4.3 Results

As seen in Figures 4.1, 4.2 showing structure factor plot of the bond correlation functions, we don't see any peaks away from the $\vec{q} = \vec{0}$ for N=6 at any temperature or at any studied lattice size. Thus, the AEA systems don't show any kind of valence bond order at $N = 6$. The results of Monte Carlo simulations show that there are no peaks away from $\vec{q} = \vec{0}$ for $N = 8$ (Figures 4.3, 4.4) or for any other value of N at any temperature and for any system size. Thus, valence bond order doesn't develop in AEA systems as a consequence of thermal fluctuations for $N = 6, 7, 8, 9, 10$.

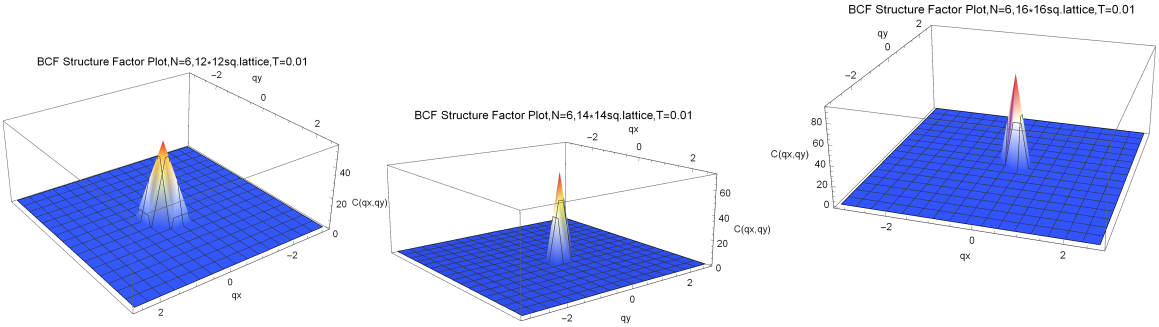

Figure 4.2: Structure factor plots for bond correlation function for N=6, T=0.01 and for various system sizes

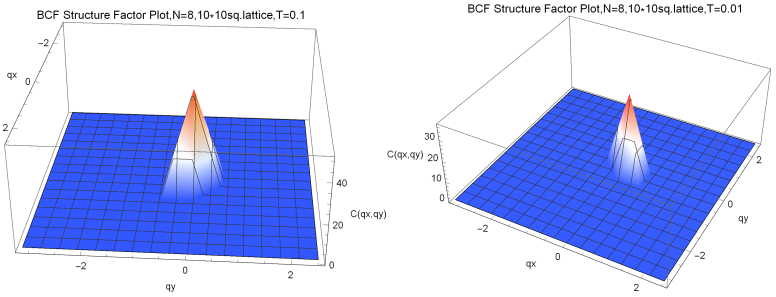

Figure 4.3: Structure factor plots for bond correlation function for N=8 and 10 by 10 lattice

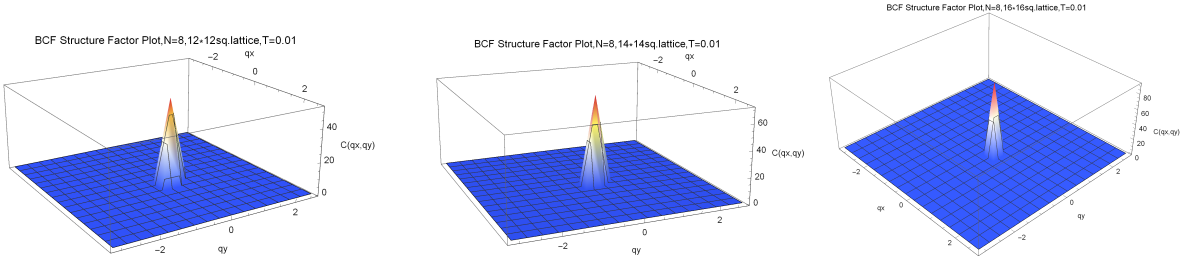

Figure 4.4: Structure factor plots for bond correlation function for N=8, T=0.01 and for various system sizes

Chapter 5

Spin Chirality and Chiral Correlation Function

5.1 Introduction

The last type of object we analyze in the AEA is the spin chirality. We also analyze the correlation between chiralities. A nonzero chirality and chiral correlation function break time reversal (τ) and parity (P) symmetry. Time reversal transformation corresponds to changing the sign of an imaginary unit ($i \to -i$). Parity transformation corresponds to flipping the sign of one of the spatial coordinates. In the case of a two dimensional lattice, we flip the sign of the x coordinate without loss of generality.

Breaking of τ and P in spin systems indicates a phase transition from paramagnetic phase to a chiral spin liquid phase. In the case of AEA model, a chiral spin liquid phase was found in the quantum model at a zero temperature as a consequence of thermal fluctuations [13].

5.2 Definition

To define spin chirality on a two dimensional lattice, we consider three spins in an arrangement like in Figure 5.1. We label each chosen spin by an integer and define

$$P_{123} = (\hat{n_{\vec{1}}}^{\dagger} \cdot \hat{n_{\vec{2}}})(\hat{n_{\vec{2}}}^{\dagger} \cdot \hat{n_{\vec{3}}})(\hat{n_{\vec{3}}}^{\dagger} \cdot \hat{n_{\vec{1}}}) \tag{5.1}$$

Having defined P_{123}, we cyclically permute indices to get P_{321} in the same manner as P_{123} and then define spin chirality as

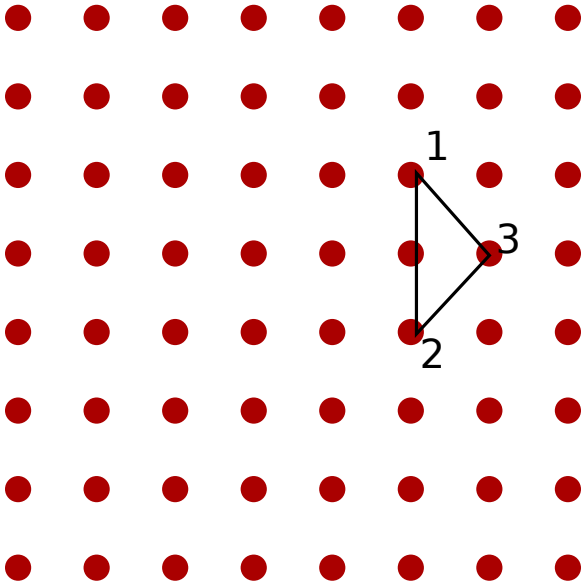

Figure 5.1: Spin chirality on a square lattice

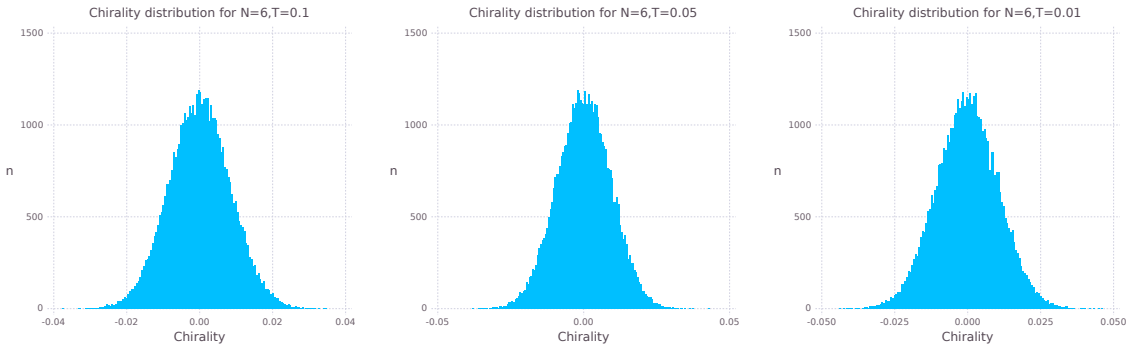

Figure 5.2: Chirality histograms for N=6 on a 10 by 10 lattice

$$C_{123} = i(P_{123} - P_{321}) \tag{5.2}$$

We can also define a chirality correlation function $C_C(\vec{r})$ as

$$C_c(\vec{r}) =< Im(C_{123}C_{1'2'3'}) > \tag{5.3}$$

where $\vec{r}$ is the distance between the sites labeled 1 and $1^{'}$. However, since the correlation function defined this way is going to be very small at low temperatures, we again normalize it. The normalized correlation function we will study is then defined as

$$C_{cc}(\vec{r}) = C_c(\vec{r})/C_c(\vec{0}) \tag{5.4}$$

5.3 Results

We present the results for the spin chirality and chirality correlation function obtained from the Monte Carlo simulations. First we present the results for the spin chirality. From the histograms shown in Figures 5.2, 5.3, we conclude that while spin chirality can take bigger absolute values at lower values of N and at lower temperatures, the expectation value of spin chirality is still zero.

Next, we analyze results for chirality correlation function(Figures 5.4, 5.5). We observe that the difference between the highest and the lowest value of the structure factor is about $\frac{1}{5}$ of the

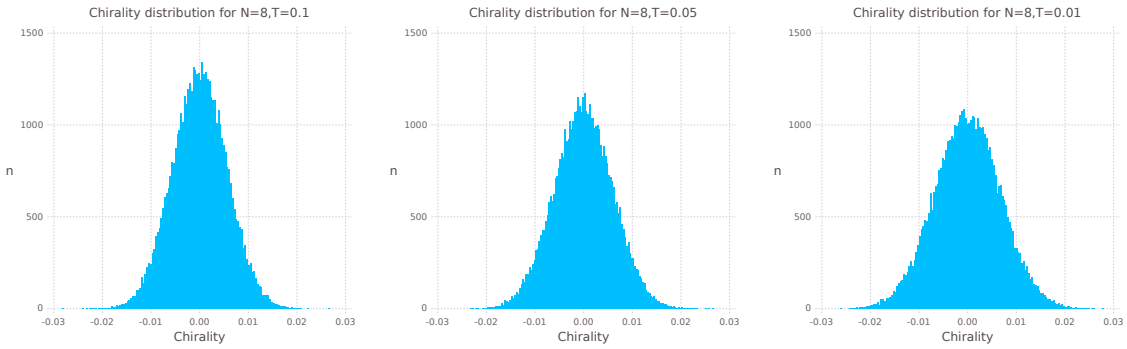

Figure 5.3: Chirality histograms for N=8 on a 10 by 10 lattice

error in structure factor (for any temperature, any system size and any value of N). Thus, no peaks develop and thus the system doesn't show chiral spin liquid order at any temperature.

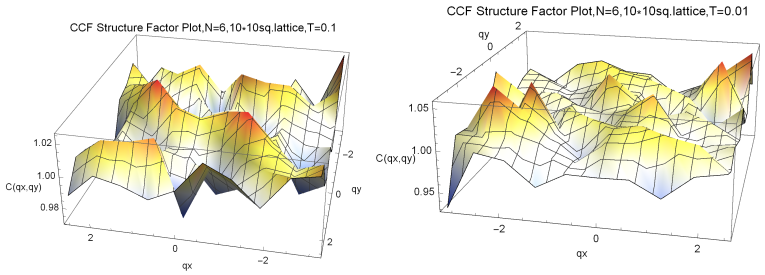

Figure 5.4: Chirality correlation function for N=6 on a 10 by 10 lattice

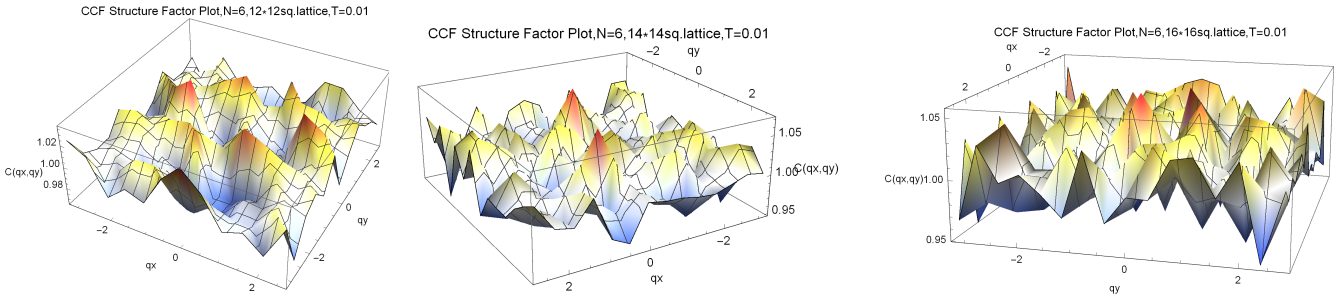

Figure 5.5: Chirality correlation function for N=6 and T=0.1 for different lattice sizes

Chapter 6

Conclusion and Future Work

The results of the Monte Carlo simulations have indicated that fermionic ultracold AEA gases don't show any sort of order as a consequence of thermal fluctuations. AEA gases in the Mott insulating limit are found in paramagnetic phase at any finite temperature.

However, the results obtained are nonetheless an indicator of direction in which further study of the influence of thermal fluctuations on behavior of AEA ultracold fermionic gases can proceed. Even though no symmetry breaking and thus no phase transitions have been found, the structure factor plots for all three correlation functions as well as the histogram for the analysis of chirality show that order is more likely to develop for lower values of N. However, to study those cases we need a new Monte Carlo algorithm. Current algorithm cannot be used to simulate behavior of AEA gases when $N = 2, 3, 4, 5$. Developing a new algorithm remains the biggest challenge for studying AEA gases with smaller values of atomic spin.

Furthermore, one can also look into AEA gases arranged into different types of lattices. The easiest one to study would be the triangular lattice, but one can also study other lattices like the pyrochlore lattice, the hexagonal lattice or the kagome lattice.

Finally, we focused our attention on the semiclassical model in a Mott insulating limit, in which one completely neglected the effects of hopping terms, as they were insignificant compared to the interaction terms. However, one can study the effects of those correction terms. Note, however, that in order to study the effects of thermal fluctuations on AEA gases in a different setup will likely require a different semiclassical model, as the derivation of the semiclassical model depends

on the quantum model in consideration.

Bibliography

[1] Ehud Altman, Eugene Demler, and Mikhail D. Lukin. Probing many-body states of ultracold atoms via noise correlations. Phys. Rev. A, 70:013603, Jul 2004.

[2] M. H. Anderson, J. R. Ensher, M. R. Matthews, C. E. Wieman, and E. A. Cornell. Observation of bose-einstein condensation in a dilute atomic vapor. Science, 269(5221):198–201, 1995.

[3] Immanuel Bloch, Jean Dalibard, and Wilhelm Zwerger. Many-body physics with ultracold gases. Rev. Mod. Phys., 80:885–964, Jul 2008.

[4] Tomas Brauner. Spontaneous symmetry breaking and nambu-goldstone bosons in quantum many-body systems. Symmetry, 2(2):609, 2010.

[5] Gia-Wei Chern and R. Moessner. Dipolar order by disorder in the classical heisenberg antiferromagnet on the kagome lattice. Phys. Rev. Lett., 110:077201, Feb 2013.

[6] Ph. Courteille, R. S. Freeland, D. J. Heinzen, F. A. van Abeelen, and B. J. Verhaar. Observation of a feshbach resonance in cold atom scattering. Phys. Rev. Lett., 81:69–72, Jul 1998.

[7] Andrew J. Daley, Martin M. Boyd, Jun Ye, and Peter Zoller. Quantum computing with alkaline-earth-metal atoms. Phys. Rev. Lett., 101:170504, Oct 2008.

[8] Thomas DeGrand and Roland Hoffmann. Qcd with one compact spatial dimension. Journal of High Energy Physics, 2007(02):022, 2007.

[9] Jeffrey Goldstone, Abdus Salam, and Steven Weinberg. Broken symmetries. Phys. Rev., 127:965–970, Aug 1962.

[10] A. V. Gorshkov, M. Hermele, V. Gurarie, C. Xu, P. S. Julienne, J. Ye, P. Zoller, E. Demler, M. D. Lukin, and A. M. Rey. Two-orbital su(n) magnetism with ultracold alkaline-earth atoms. Nat Phys, 6(4):289–295, Apr 2010.

[11] A. K. Hartmann and H. Rieger. New Optimization Algorithms in Physics. Wiley-VCH Verlag GmbH and Co. KGaA, 2004.

[12] Michael Hermele and Victor Gurarie. Topological liquids and valence cluster states in two-dimensional su(n) magnets. Phys. Rev. B, 84:174441, Nov 2011.

[13] Michael Hermele, Victor Gurarie, and Ana Maria Rey. Mott insulators of ultracold fermionic alkaline earth atoms: Underconstrained magnetism and chiral spin liquid. Phys. Rev. Lett., 103:135301, Sep 2009.

[14] Julia website. url "http://julialang.org/".

[15] J. Kertesz and I. Kondor. Advances in Computer Simulation. Springer Verlag, 1998.

[16] Aslam Parvej Manoranjan Kumar and Z.G. Soos. Spin structure factor and quantum phases of frustrated spin-1/2 chains. arXiv:1405.1578, 2014.

[17] R. Moessner and J. T. Chalker. Properties of a classical spin liquid: The heisenberg pyrochlore antiferromagnet. Phys. Rev. Lett., 80:2929–2932, Mar 1998.

[18] Roderich Moessner. Magnets with strong geometric frustration. Can. J. Phys, 79:1283, 2001.

[19] C. A. Regal, M. Greiner, and D. S. Jin. Observation of resonance condensation of fermionic atom pairs. Phys. Rev. Lett., 92:040403, Jan 2004.

[20] Shu Tanaka and Seiji Miyashita. Slow relaxation of spin structure in exotic ferromagnetic phase of ising-like heisenberg kagome antiferromagnets. Journal of the Physical Society of Japan, 76(10):103001, 2007.

[21] Villain, J., Bidaux, R., Carton, J.-P., and Conte, R. Order as an effect of disorder. J. Phys. France, 41(11):1263–1272, 1980.

[22] Kun Yang. Spontaneous symmetry breaking and quantum hall effect in graphene. Solid State Communications, 143(1-2):27 – 32, 2007. Exploring graphene;Recent research advances.